

Integrated Sensing and Communication for Large Networks using a Dynamic Transmission Strategy and Full Duplex

Konpal Shaukat Ali and Marwa Chafii

Abstract—A large network employing integrated sensing and communication (ISAC) where a single transmit signal by the base station (BS) serves both the radar and communication modes is studied. Typically in ISAC, bistatic radar detection is done at a passive radar. The radar-mode performance is significantly more vulnerable than the communication-mode due to the double path-loss in the signal component while interferers have direct links. To combat this, we propose: 1) monostatic radar detection at the BS via full-duplex (FD), 2) a novel dynamic transmission strategy (DTS). With FD monostatic detection we are able to improve radar-mode performance over bistatic detection in certain scenarios, while bistatic detection dominates in others. We also analyze the performance of joint bistatic and FD monostatic detection. Significant improvements in radar-performance can be attained with joint detection in certain scenarios, while using one strategy is beneficial in others. Our results highlight that with the DTS we are able to significantly improve quality of radar detection at the cost of quantity. Further, DTS causes some performance deterioration to the communication-mode; however, the gains attained for the radar-mode are much higher. We show that joint detection and DTS together can significantly improve radar performance from a traditional radar-network.

Index Terms—Integrated sensing and communication (ISAC), stochastic geometry, full duplex

I. INTRODUCTION

There is an ever increasing need for connectivity which in next generation networks will not only mean growing communication requirements like higher throughput and reliability but also increased sensing requirements. A number of applications such as vehicle-to-vehicle communication, drones, smart cities and more generally the internet of things (IoT) have both high communication and sensing requirements [1], [2]. Although radar sensing and communication share a lot in terms of both software and hardware, for decades, the two have been advancing independently with limited intersection [1], [2]. Since the wireless spectrum is scarce, it is natural to consider systems that are able to ‘reuse’ the spectrum more efficiently and utilize it for both communication and sensing simultaneously.

In this work, we use *integrated sensing and communication* (ISAC) to refer to a system that jointly designs and uses a *single* transmit signal for both communication and sensing. Such systems have also been referred to by names such as joint radar and communication (JRC), joint communication

and radar (JCR), joint communication and radar/radio sensing (JCAS), radar-communication (RadCom) and dual-function radar communications (DFRC) [1]. ISAC offers improved spectral efficiency and reduced hardware costs [3]. Further, in contrast to coexisting communication and sensing systems where a single transmit signal does not serve both the radar and communication-modes, ISAC also protects the network from additional interference.

The majority of work on ISAC has focused on setups with a single-cell/few cells [4]–[6]. Since real networks are becoming very dense and have high interference, studying such setups can lead to inaccurate deductions as well as result in suboptimum parameter selection that can hurt performance in a real network [7]. Studying a large network that mimics a real-world network is thus of great value. Stochastic geometry provides a unified mathematical paradigm for modeling large wireless networks and characterizing their operation while taking intercell interference into account [8], [9]. Works such as [3], [10]–[12] have studied coexisting communication and sensing using stochastic geometry tools; however, these setups were not ISAC as the same transmit signal was not used by the radar and communication-modes simultaneously. In [10] a network where nodes shared a channel to work in the radar and communication-modes in different time slots was studied. The impact of only the strongest interferer was considered, thus the interference from the entire network was not accounted for. In [11] multi-radar cooperative detection was used to enhance the detection range by clusters of radars sharing their sensing information via the communication-mode. It was also assumed that the radar-mode does not receive interference from both the communication and radar-modes. In [12] a 1D setup of vehicles was studied where communication and radar were on different bandwidths. As a vehicle is unable to detect targets outside of its self-detection range, the goal of the work was to use cooperation between vehicles to increase the detection range. Interference from the network was not considered. In [3] a bistatic setup was studied where the transmitting base station (BS) and detecting radar were at fixed locations while multiple users (UEs) and clutter scatterers were distributed according to a Poisson point process (PPP). The BS served the radar and communication functionalities in a time division manner. The goal was to optimize the network throughput. On the other hand, works such as [4]–[6] study ISAC where a single transmit signal is shared by the two modes in the same frequency channel simultaneously; however, these works do not consider a large network. To

The authors are with the Engineering Division, New York University (NYU) Abu Dhabi, 129188, UAE (Email: {konpal.ali, marwa.chafii}@nyu.edu). M. Chafii is also with NYU WIRELESS, NYU Tandon School of Engineering, Brooklyn, 11201, NY.

the best of our knowledge, a study on the impact of ISAC, where both the radar and communication-modes share a single transmit signal and operate in the same frequency channel simultaneously, in a large network does not exist.

Radar sensing can be done via monostatic detection, i.e., the transmitter of the signal detects the echo, if any, as well as via bistatic detection where the transmitter is not collocated with the radar receiver. In the ISAC network the cellular BS transmits a signal that is also used by the radar-mode. Thus, bistatic detection is more common in ISAC networks since it is convenient to deploy many low-cost passive radars for listening, as the radar-mode utilizes the communication-mode's spectrum as well as the transmit power. Monostatic detection at the BS is also a possibility; this, however, requires full duplex (FD) operation as the BS simultaneously transmits and receives on the same channel. While simultaneously transmitting and receiving messages on the same channel was not possible previously due to the the overwhelming self-interference (SI), with recent advances in transceiver design, successful SI cancellation (SIC) is now possible that enables FD operation. Thus, using SIC, a transceiver is able to simultaneously transmit and receive on the same frequency channel, i.e., operate in FD [13], [14]. A number of works exist on FD [15] and in [16] FD operation was identified as a key enabler for such ISAC systems.

The radar-mode is particularly vulnerable as its signal component suffers a double path loss (both in the FD monostatic and bistatic case) due to the nature of radar detection. Further, in a large network, the receiver in the radar-mode still incurs interference from all the nodes in the network directly, which do not undergo a double path loss effect. These two factors play a significant role in deteriorating the signal to interference and noise ratio (SINR) of the radar-mode. The communication-mode, on the other hand, is 'safe' as it does not incur deterioration compared to a regular cellular network without ISAC.

In this work we study a large network where the radar and communication modes share a single transmit signal and operate in the same frequency channel simultaneously. We take into account both fading and intercell interference. In light of the significant deterioration to the SINR of the radar-mode, in addition to the traditional bistatic radar detection, we propose two solutions to improve the radar-mode's performance without significantly hurting the communication-mode: 1) monostatic detection at the BS via FD, 2) a novel *dynamic transmission strategy (DTS)* for ISAC. Since the cellular BS has strong compute power and back-haul connections, we also propose the use of joint detection which involves cooperation between the bistatic and FD monostatic detection; thus, detection by either one of the approaches results in successful detection of the radar-mode. The contributions of this work can be summarized as follows:

- We propose using FD monostatic detection for the radar-mode as well as joint detection using both bistatic and FD monostatic detection.
- The DTS is proposed as a novel strategy where each BS dynamically transmits with high power in one of M slots while the remaining slots have lower power

transmissions. While communication takes place in all M slots, by limiting radar-mode detection to the slot with high power, both the signal is improved and interference power is reduced for the radar-mode. This way we trade the *quantity* of radar-mode detection for *quality*.

- We provide a tractable analytical framework to quantify the performance of the communication-mode, the radar-mode with bistatic detection, with FD monostatic detection, as well as with joint detection.
- We show that while in some scenarios, such as cell-center targets, FD monostatic is superior to bistatic detection, in other cases bistatic detection is superior. Further, when one of bistatic and monostatic detection is not significantly superior to the other, using the joint detection results in non-trivial performance improvement.
- We find that while, as anticipated, the DTS hurts the communication-mode due to increased interference in the low power slots, this deterioration is much less than the gains attained by the radar-mode from DTS.
- We show that with careful DTS parameter selection, the deterioration of the communication-mode can be reduced while improving the performance of the radar-mode.
- We benchmark the performance of the ISAC network's radar-mode with a network deploying the radar-mode only. We find that the DTS and joint detection significantly improve performance from that of a traditional radar-only network. These are thus important solutions to improve the performance of the radar-mode in ISAC.

The rest of the paper is organized as follows: Section II describes the system model. The proposed DTS and methodology of analysis is in Section III. The SINR analysis is in Section IV. Section V presents the results and Section VI concludes the paper.

Notation: We denote vectors using bold text, $\|\mathbf{z}\|$ is used to denote the Euclidean norm of the vector \mathbf{z} . The ordinary hypergeometric function is denoted by ${}_2F_1$. The cdf (ccdf, pdf) of the RV X is denoted by F_X (\bar{F}_X , f_X). The Laplace transform (LT) of the pdf of the RV X is denoted by $\mathcal{L}_X(s) = \mathbb{E}[e^{-sX}]$.

II. SYSTEM MODEL

A. ISAC Network Model

We consider a downlink cellular network where BSs are distributed according to a homogeneous PPP Φ with intensity λ . We assume communication-mode UEs are distributed uniformly and independently at random in the cells. Additionally, there are radar-mode targets and radars present in the network. The radars can listen for the echo of the relevant target in the cell they are in. In this work we consider both bistatic detection at the radar and monostatic detection at the BS via FD. The performance of bistatic and FD monostatic detection is analyzed separately and we also analyze the impact of joint detection via both techniques. A BS assigns each UE in its cell a unique time-frequency resource block to avoid interference between the messages of UEs in a cell. At the same time, in an effort to reuse the spectrum for sensing as well, the BS uses the communication signal to probe and sense the target at an unknown location inside the cell. This way,

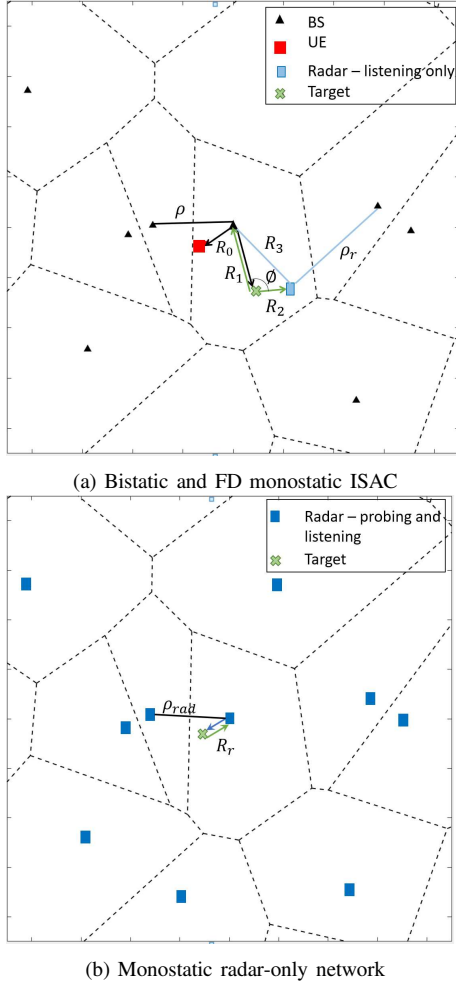


Fig. 1: A snapshot realization of the network. All the nodes of interest in the typical cell have been shown.

using ISAC, additional resources are not spent for detection in the radar-mode. Note that radars in the radar-mode do not transmit probing signals in the ISAC setup to avoid additional interference to the communication-mode; thus the radar-mode is allowed to use the communication-mode's spectrum for free without hurting the communication-mode. We assume that the radar in bistatic detection has knowledge of the probing signal from the BS; thus, a radar only detects targets inside the cell of the BS it is in. We also assume the BS is equipped with FD capability for monostatic detection.

To the network we add a BS at the origin \mathbf{o} , which, under expectation over Φ , becomes the typical BS (tBS) serving the typical UE (tUE) in the typical cell. The echo of the tBS's message from the typical target (tTar) is listened for at the typical radar (tRad) in bistatic detection and at the tBS itself via FD in the case of monostatic detection. In the remainder of this work, we study the performance of the typical cell. Since Φ does not include the BS at \mathbf{o} , the set of interfering BSs for the tUE is Φ . As the tRad is aware of the message of the tBS, this is canceled and removed; thus, the set of interfering BSs for the tRad in the case of bistatic detection is also Φ . Also, naturally, the set of interfering BSs at the tBS in the case of monostatic detection via FD is also Φ . Fig. 1a is a

snapshot of the ISAC network where the nodes in the typical cell are shown. The tUE (tRad) lies a distance R_0 (R_3) from the tBS at \mathbf{o} . The tTar lies a distance R_1 from the tBS at \mathbf{o} . The tRad attempting to detect tTar lies a distance R_2 from it. The distance between the tBS (tRad) and its nearest interferer is denoted by ρ (ρ_r).

B. Radar-only Network Model

In order to compare and benchmark the performance of our ISAC system, we introduce a radar-only network where the radars do not share communication spectrum. Here the radars are distributed according to a PPP Φ_r with intensity λ . Monostatic radars are considered as it is assumed that radars cannot communicate with each other to cooperate due to a lack of the kind of infrastructure BSs have. Thus, a radar attempts to detect a target inside its cell by sending a probing signal with power P_r and listening for its reflected signal. In contrast to the ISAC network, the radar-mode does not deal with interference from the PP of BSs; however, interference from the PP of radars sending probing signals exists.

Similar to the ISAC setup, we add a radar at the origin \mathbf{o} , which under expectation over Φ_r becomes the tRad searching for the tTar in the typical cell. Since Φ_r does not include the radar at \mathbf{o} , the set of interfering radars for the tRad is Φ_r . Fig. 1b shows a snapshot of the radar-only network. The tTar lies a distance R_r from the tRad at \mathbf{o} , and the distance between the tRad and its nearest interferer is denoted by ρ_{rad} .

C. Channel Model and Link Distance Distribution

We assume a Rayleigh fading environment such that the fading coefficient between any two nodes is i.i.d. with a unit mean exponential distribution. A power-law path loss model is considered where the signal decays at the rate $r^{-\eta}$ with distance r , $\eta > 2$ denotes the path loss exponent and $\delta = \frac{2}{\eta}$.

In the ISAC network the UEs are distributed uniformly and randomly in the cells and the BSs are distributed according to a PPP with intensity λ . Accordingly, the distribution of the link distance R_0 follows

$$f_{R_0}(x) = 2\pi b \lambda x \exp(-\pi b \lambda x^2), \quad x \geq 0,$$

where $b = 13/10$ is the correction factor due to the fact that the nodes of interest are in the typical cell, not in the 0-cell [17, (12)].

In the ISAC network, we assume the tTar (tRad) lies a fixed distance $R_1 = r_1$ ($R_2 = r_2$) away from the tBS (tTar) in a random direction. The angle between the tBS-tTar link and the tTar-tRad link, as shown in Fig. 1a, is denoted by ϕ and follows the distribution $f_\phi(u) = 1/(2\pi)$, $0 \leq u \leq 2\pi$. As a result, the distance between the tRad and tBS at \mathbf{o} , denoted by R_3 , is

$$R_3 = \sqrt{r_1^2 + r_2^2 - 2r_1r_2 \cos \phi}. \quad (1)$$

Proposition 1: The distribution of the link distance R_3 is accurately approximated as

$$F_{R_3}(r) \approx \frac{1}{\pi} \cos^{-1} \left(\frac{-(r - |r_1 - r_2| - \min(r_1, r_2))}{\min(r_1, r_2)} \right), \quad (2)$$

$$f_{R_3}(r) \approx \frac{1}{\pi \min(r_1, r_2)} \frac{1}{\sqrt{\left(1 - \left(1 + \frac{|r_1 - r_2| - r}{\min(r_1, r_2)}\right)^2\right)}},$$

$$|r_1 - r_2| \leq r \leq r_1 + r_2. \quad (3)$$

Proof: From Fig. 1a and (1), $|r_1 - r_2| \leq R_3 \leq r_1 + r_2$. Based on the uniform distribution of ϕ in $[0, 2\pi]$, we plot the exact distribution of R_3 in Fig. 2 via simulations. The cdf is infinitely steep on both ends of the support and in the middle (at $\max(r_1, r_2)$) the value is close to 0.5 since the cdf is almost symmetric. This distribution is accurately modeled by taking the inverse of a scaled and translated cosine function as follows

$$r = \min(r_1, r_2) (1 - \cos(\pi F_{R_3}(r))) + |r_1 - r_2|.$$

By inverting this expression, we obtain the approximate cdf $F_{R_3}(r)$ in (2). From Fig. 2 we observe that for different values of r_1 and r_2 , the approximate analysis in (2) matches the actual cdf of R_3 obtained via simulations closely, thus justifying the use of this approximation. The corresponding pdf $f_{R_3}(r)$ in (3) is easily obtained by taking the derivative of (2). \square

Remark 1: $F_{R_3}(r)$ is unchanged if the values of r_1 and r_2 are interchanged as this means the positions of the BS and radar in Fig. 1a have been swapped.

In the radar-only network, we assume that the tTar lies a distance $R_r = r_r$ from the tRad in a random direction.

Due to the PPP nature of the interferers in both the ISAC network and radar-only network, the distance of the tBS in the ISAC network to its nearest interferer, ρ , and the distance of the tRad in the radar-only network to its nearest interferer, ρ_{rad} , follow:

$$f_\chi(r) = 2\pi\lambda r \exp(-\pi\lambda r^2), \quad r \geq 0, \quad (4)$$

where $\chi \in \{\rho, \rho_{\text{rad}}\}$.

In the ISAC network, the distance between the tRad and its nearest interferer, ρ_r conditioned on R_3 follows

$$f_{\rho_r|R_3}(r | R_3) = 2\pi\lambda r \exp(-\pi\lambda(r^2 - R_3^2)), \quad r \geq R_3, \quad (5)$$

due to the PPP distribution of interferers and the fact that the interferer lies greater than a distance R_3 away from the tRad¹.

III. PROPOSED STRATEGY AND ANALYSIS METHODOLOGY

A. Dynamic Transmission Strategy (DTS) for ISAC

In the radar-mode of ISAC, the signal received at the radar and BS (in bistatic and FD monostatic detection, respectively) is significantly weaker than the signal received by communication-mode users due to the double path loss associated with the signal in the radar-mode first going from the BS to the target and then from the target to the radar and BS. In contrast to the double path loss in the signal component of the radar-mode, the interference received at the radar and BS comes via direct links from interfering BSs; this

¹Since this work uses fixed distances $R_1 = r_1$ and $R_2 = r_2$ (to see the impact of varying these distances on radar-mode performance), we conditioned the distribution of ρ_r on R_3 (a function of r_1 and r_2) for better accuracy of the statistics of ρ_r .

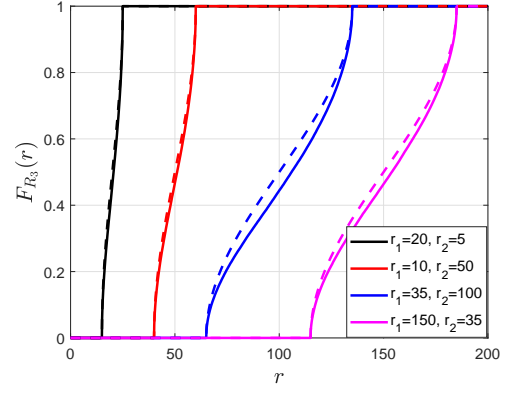


Fig. 2: The cdf of R_3 for different values of r_1 and r_2 . Solid lines represent the simulations while dashed lines are used for the approximation in (2).

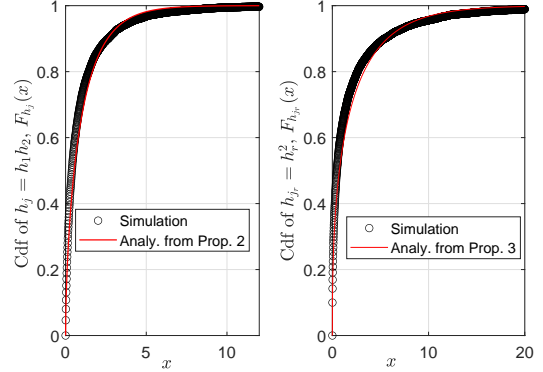


Fig. 3: The simulated and proposed analytical cdf of h_j and h_{jr} in (6) and (7), respectively.

further deteriorates the radar-mode's SINR. To combat this, we propose a transmission strategy referred to as the DTS in which BSs transmit with high power P_h in one slot and with regular lower power P_l in the remaining $M - 1$ slots, where $M \geq 2$. The slot in which a BS transmits with higher power is chosen in an ALOHA fashion for different BSs and this is the slot in which the radar-mode is also active, i.e., ISAC takes place. The communication-mode, on the other hand, is active in all M slots. For notational convenience, we refer to the slot in which the tBS transmits with P_h as 'slot 1'. Such a transmission strategy allows us to control the average network interference for both the communication and radar-modes as the probability of an interferer transmitting with P_h is $1/M$. It also simultaneously gives the more vulnerable radar-mode, which is only active in slot 1, a higher transmission power to help improve its signal that undergoes a double path loss. Thus, the average radar signal power P_h is higher than the average interference power, $P_{\text{avg}} = (P_h + (M - 1)P_l)/M$.

This way we are able to improve the SINR of the radar-mode while having control on the impact it has on the communication-mode. Note, however, that the price paid is reduced sensing as detection in the radar-mode only happens $1/M$ of the time. Since the communication requirements are generally much higher than sensing requirements and the radar-mode rides for free in the communication-mode's spectrum, the price paid is reasonable. Further, while the

average signal power of the communication-mode is also P_{avg} , the precise impact of this dynamic transmission strategy on the communication-mode is not obvious; we will thus also analyze it in this work. We study the performance of both the communication-mode and radar-mode over M time slots and assume that the tBS serves the tUE for M time slots.

It ought to be noted that while ISAC is promoted for more efficient use of the spectrum, which is a scarce resource, and reduced network power consumption (via fewer transmissions), the interference encountered by the nodes, including the communication-mode user, is higher with DTS than without DTS as $P_{\text{avg}} > P_l$. Since the communication-mode typically pays for this in terms of resources (spectrum and transmit power) and since the DTS can negatively impact the communication mode due to increased interference from the scenario without DTS, protecting the communication-mode is a priority.

B. Methodology of Analysis

Fixed-rate transmissions are used in this work, such that a message is sent with transmission rate $\log(1+\theta)$ corresponding to an SINR threshold of θ . Such transmissions result in a throughput that is lower than the transmission rate because of possible outages. The performance of the communication-mode is typically measured using the coverage probability (i.e., the SINR cdf), which is a measure of reliability, and throughput. Radar performance was traditionally analyzed using metrics like the detection probability and faulty error probability. More recently, however, works on ISAC such as [4], coexisting communication and radar [3] and even radar only [18], [19] have switched to analyzing the performance of the radar-mode using the statistics of the SNR or SINR. In this work, we also focus on analyzing radar-mode performance using the statistics of the SINR at the radar and BS (in the bistatic and FD monostatic cases, respectively) as a measure of reliable detection.

IV. SINR ANALYSIS

A. Preliminaries

The fading coefficient between the tBS at \mathbf{o} and the tUE (tTar) at \mathbf{c} (\mathbf{t}) is h_0 (h_1), and between the tTar and the tRad at \mathbf{r} is h_2 . As the signal in the bistatic radar-mode goes from the tBS to the tTar and then to the tRad, the joint fading experienced at the tRad is $h_j = h_1 h_2$. On the other hand, in the FD monostatic radar-mode, the signal goes from the tBS to the tTar and then back to the tBS; the joint fading experienced at the tBS is $h_{j_r} = h_1^2$. Due to the Rayleigh fading assumption, h_0 , h_1 and h_2 are independent unit mean exponential RVs.

While the exact statistics of the joint fading RVs h_j and h_{j_r} can be obtained, these approaches do not lead to tractability in obtaining the statistics of the SINR for the bistatic and FD monostatic radar-mode which we are interested in. We thus propose the use of tight approximations through curve fitting for the statistics of h_j and h_{j_r} that will allow tractability in obtaining the SINR statistics.

Proposition 2: The cdf of the unit mean RV h_j is approximated using

$$F_{h_j}(x) = (1 - \exp(-\epsilon y))^m, \quad (6)$$

where $m = \sqrt{7/20}$ and $\epsilon = \text{harmonic}(m)$.

Proof: Based on the lower bound of the cdf of a gamma RV [20], which is in a form that allows tractability in obtaining the statistics of the SINR for a PPP of interferers, using the fact that $\mathbb{E}[h_j] = \mathbb{E}[h_1]\mathbb{E}[h_2] = 1$ and via fitting we obtain the expression in (6). In Fig. 3 we observe that the exact distribution based on simulations closely matches the analytical approximate in (6). \square

Proposition 3: The cdf of the RV h_{j_r} with $\mathbb{E}[h_{j_r}] = 2$ is approximated using

$$F_{h_{j_r}}(x) = (1 - \exp(-\epsilon_r y))^{m_r}, \quad (7)$$

where $m_r = \sqrt{3/20}$ and $\epsilon_r = \text{harmonic}(m)/2$.

Proof: Along the lines of the proof of Proposition 2 and using the fact that $\mathbb{E}[h_{j_r}] = \mathbb{E}[h_1^2] = \text{Var}(h_1) + (\mathbb{E}[h_1])^2 = 2$ as $h_1 \sim \exp(1)$, we obtain (7). In Fig. 3 we observe that the exact distribution based on simulations closely matches the analytical approximate in (7). \square

The intercell interference experienced at a receiver located at \mathbf{z} scaled to unit transmission power is of the form

$$I_z = \sum_{\mathbf{x} \in \Phi} g_{\mathbf{x}_z} \|\mathbf{x} - \mathbf{z}\|^{-\eta}, \quad (8)$$

where $z \in \{c, r, o\}$ denotes the interference at \mathbf{c} , \mathbf{r} and \mathbf{o} in the cellular mode, bistatic radar-mode and FD monostatic radar-mode, respectively. Here, $g_{\mathbf{x}_z}$ denotes the fading coefficient from the interfering BS at \mathbf{x} to the receiver at \mathbf{z} .

For the case of $z \in \{r, o\}$, i.e., the bistatic and monostatic radar modes, let ψ denote the distance between the receiver and the nearest interferer, where $\psi = \{\rho_r, \rho\}$ for the bistatic and FD monostatic radar-modes, respectively. The intercell interference for $z \in \{r, o\}$ scaled to unit transmission power at \mathbf{z} can be rewritten as

$$I_z = \sum_{\substack{\mathbf{x} \in \Phi \\ \|\mathbf{x} - \mathbf{z}\| > \psi}} g_{\mathbf{x}_z} \|\mathbf{x} - \mathbf{z}\|^{-\eta} + \sum_{\substack{\mathbf{x} \in \Phi \\ \|\mathbf{x} - \mathbf{z}\| = \psi}} g_{\mathbf{x}_z} \|\mathbf{x} - \mathbf{z}\|^{-\eta}, \quad (9)$$

The LT of I_z for $z \in \{r, o\}$ conditioned on ψ is given by

$$\mathcal{L}_{I_z|\psi}(s) = \exp\left(\frac{-2\pi\lambda s}{(\eta-2)\psi^{\eta-2}} {}_2F_1\left(1, 1-\delta; 2-\delta; \frac{-s}{\psi^\eta}\right)\right) \frac{1}{1+s\psi^{-\eta}} \quad (10)$$

$$\stackrel{\eta=4}{=} \exp\left(-\pi\lambda\sqrt{s}\tan^{-1}\left(\sqrt{s}\psi^{-2}\right)\right) \frac{1}{1+s\psi^{-\eta}}. \quad (11)$$

We obtain the first term in (10) using the probability generating functional (pgfl) of the PPP, the guard zone distance ψ and the fact that $g_{\mathbf{x}_z} \sim \exp(1)$ due to the Rayleigh fading assumption [21]. The second term in (10) comes from $g_{\mathbf{x}_z} \sim \exp(1)$ and due to the fact that an interferer is conditioned to exist at a distance ψ from the receiver according to the second term in (9).

The LT of I_c , the intercell interference in the communication-mode at the tUE located at \mathbf{c} scaled to

unit transmission power, conditioned on the link distance R_0 is

$$\mathcal{L}_{I_c|R_0}(s) = \exp\left(\frac{-2\pi\lambda s}{(\eta-2)R_0^{\eta-2}} {}_2F_1\left(1, 1-\delta; 2-\delta; \frac{-s}{R_0^\eta}\right)\right) \quad (12)$$

$$\stackrel{\eta=4}{=} \exp\left(-\pi\lambda\sqrt{s}\tan^{-1}\left(\sqrt{s}R_0^{-2}\right)\right) \quad (13)$$

Similar to (10), we obtain (12) using the pgfl of the PPP, the guard zone distance R_0 and the fact that $g_{x_z} \sim \exp(1)$.

B. SINR Analysis of ISAC Network employing the DTS

The SINR of the communication-mode at the tUE in an ISAC network employing the DTS when the tBS transmits with power P_χ , $\chi \in \{l, h\}$, is

$$\text{SINR}_c^\chi = \frac{P_\chi h_0 R_0^{-\eta}}{P_{\text{avg}} I_c + \sigma^2}. \quad (14)$$

The interference experienced at the tUE located at \mathbf{c} is $P_{\text{avg}} I_c$.

Lemma 1: The ccdf of the communication-mode SINR when the tBS transmits with power P_χ , $\chi \in \{l, h\}$ in an ISAC network employing DTS is

$$\begin{aligned} \mathbb{P}(\text{SINR}_c^\chi > \theta) &= \mathbb{E}\left[\bar{F}_{h_0}\left(\frac{\theta R_0^\eta}{P_\chi}(P_{\text{avg}} I_c + \sigma^2)\right)\right] \\ &= \mathbb{E}_{R_0}\left[\mathcal{L}_{I_c|R_0}\left(\frac{\theta R_0^\eta P_{\text{avg}}}{P_\chi}\right) \exp\left(\frac{-\theta R_0^\eta \sigma^2}{P_\chi}\right)\right], \end{aligned} \quad (15)$$

where $\mathcal{L}_{I_c|R_0}(s)$ is given in (12).

Proof: Rewriting the SINR expression in (14) and since $h_0 \sim \exp(1)$, using the definition of the LT, we obtain (15). \square

Corollary 1: The average ccdf of the communication-mode SINR in an ISAC network employing DTS is

$$\mathbb{P}(\text{SINR}_c^{\text{avg}} > \theta) = \frac{1}{M} \mathbb{P}(\text{SINR}_c^h > \theta) + \frac{M-1}{M} \mathbb{P}(\text{SINR}_c^l > \theta). \quad (16)$$

The SINR of the bistatic radar-mode at the tRad in an ISAC network employing the DTS is

$$\text{SINR}_{r,b} = \frac{P_h h_1 h_2 r_1^{-\eta} r_2^{-\eta}}{P_{\text{avg}} I_r + \sigma^2} = \frac{P_h h_j r_1^{-\eta} r_2^{-\eta}}{P_{\text{avg}} I_r + \sigma^2}. \quad (17)$$

The interference experienced at the tRad located at \mathbf{r} is $P_{\text{avg}} I_r$.

Lemma 2: The ccdf of the bistatic radar-mode's SINR in an ISAC network employing DTS is

$$\begin{aligned} \mathbb{P}(\text{SINR}_{r,b} > \theta) &= \mathbb{E}\left[\bar{F}_{h_j}\left(\frac{\theta r_1^\eta r_2^\eta}{P_h}(P_{\text{avg}} I_r + \sigma^2)\right)\right] \\ &= 1 - \mathbb{E}_{R_3, \rho_r}\left[\left(1 - \mathcal{L}_{I_r|\rho_r}\left(\frac{\epsilon \theta r_1^\eta r_2^\eta P_{\text{avg}}}{P_h}\right) \exp\left(\frac{-\epsilon \theta r_1^\eta r_2^\eta \sigma^2}{P_h}\right)\right)^m\right], \end{aligned} \quad (18)$$

where $\mathcal{L}_{I_r|\rho_r}(s)$ is obtained from (10).

Proof: Rewriting the SINR expression in (17) and using the cdf of h_j in (6) along with the definition of the LT, we obtain (18). \square

The SINR of the FD monostatic radar-mode at the tBS in an ISAC network employing the DTS is

$$\text{SINR}_{r,m} = \frac{P_h h_1 h_1 r_1^{-2\eta}}{P_{\text{avg}} I_o + \sigma^2} = \frac{P_h h_{j_r} r_1^{-2\eta}}{P_{\text{avg}} I_o + \sigma^2}. \quad (19)$$

The interference experienced at the tBS located at \mathbf{o} is $P_{\text{avg}} I_o$.

Lemma 3: The ccdf of the FD monostatic radar-mode's SINR in an ISAC network employing DTS is

$$\begin{aligned} \mathbb{P}(\text{SINR}_{r,m} > \theta) &= \mathbb{E}\left[\bar{F}_{h_{j_r}}\left(\frac{\theta r_1^{2\eta}}{P_h}(P_{\text{avg}} I_o + \sigma^2)\right)\right] \\ &= 1 - \mathbb{E}_\rho\left[\left(1 - \mathcal{L}_{I_o|\rho}\left(\frac{\epsilon_r \theta r_1^{2\eta} P_{\text{avg}}}{P_h}\right) \exp\left(\frac{-\epsilon_r \theta r_1^{2\eta} \sigma^2}{P_h}\right)\right)^{m_r}\right], \end{aligned} \quad (20)$$

where $\mathcal{L}_{I_o|\rho}(s)$ is obtained from (10).

Proof: Rewriting the SINR expression in (19) and using the cdf of h_{j_r} in (7) along with the definition of the LT, we obtain (20). \square

Corollary 2: The joint SINR ccdf of the radar-mode in an ISAC network employing DTS, where there is cooperation between bistatic and FD monostatic detection is

$$\begin{aligned} \mathbb{P}(\text{SINR}_{r,\text{joint}} > \theta) &= \mathbb{P}(\text{SINR}_{r,b} > \theta) + \mathbb{P}(\text{SINR}_{r,m} > \theta) - \\ &\quad \mathbb{P}(\text{SINR}_{r,b} > \theta) \mathbb{P}(\text{SINR}_{r,m} > \theta). \end{aligned} \quad (21)$$

Proof: From the law of probability and independence of the two detection events (21) follows. \square

C. SINR Analysis of ISAC Network without DTS

Since the proposed DTS uses the higher P_h in 1 slot, the normal transmission power in the network without DTS is P_l .

The SINR of the communication-mode at the tUE in an ISAC network without the DTS is

$$\text{SINR}_c^{\text{no DTS}} = \frac{P_l h_0 R_0^{-\eta}}{P_l I_c + \sigma^2}. \quad (22)$$

Lemma 4: The ccdf of the communication-mode SINR in an ISAC network without DTS is

$$\begin{aligned} \mathbb{P}(\text{SINR}_c^{\text{no DTS}} > \theta) &= \mathbb{E}\left[\bar{F}_{h_0}\left(\frac{\theta R_0^\eta}{P_l}(P_l I_c + \sigma^2)\right)\right] \\ &= \mathbb{E}_{R_0}\left[\mathcal{L}_{I_c|R_0}\left(\theta R_0^\eta\right) \exp\left(\frac{-\theta R_0^\eta \sigma^2}{P_l}\right)\right], \end{aligned} \quad (23)$$

where $\mathcal{L}_{I_c|R_0}(s)$ is given in (12).

Proof: Using (22) and along the lines of the proof of Lemma 1, we obtain (23).

Remark 2: The SINR of the communication-mode in a network without ISAC, i.e., a traditional cellular network, is identical to the SINR of the communication-mode in an ISAC network without DTS as the communication-mode is not impacted when DTS is not used.

The SINR of the bistatic radar-mode at the tRad in an ISAC network without the DTS is

$$\text{SINR}_{r,b}^{\text{no DTS}} = \frac{P_l h_j r_1^{-\eta} r_2^{-\eta}}{P_l I_r + \sigma^2}. \quad (24)$$

Lemma 5: The ccdf of the bistatic radar-mode's SINR in an ISAC network without DTS is

$$\begin{aligned} \mathbb{P}(\text{SINR}_{r,b}^{\text{no DTS}} > \theta) &= \mathbb{E} \left[\bar{F}_{h_j} \left(\frac{\theta r_1^\eta r_2^\eta}{P_l} (P_l I_r + \sigma^2) \right) \right] \\ &= 1 - \mathbb{E}_{R_3, \rho_r} \left[\left(1 - \mathcal{L}_{I_r | \rho_r} (\epsilon \theta r_1^\eta r_2^\eta) \exp \left(\frac{-\epsilon \theta r_1^\eta r_2^\eta \sigma^2}{P_l} \right) \right)^m \right], \end{aligned} \quad (25)$$

where $\mathcal{L}_{I_r | \rho_r}(s)$ is obtained from (10).

Proof: Using (24) and along the lines of the proof of Lemma 2, we obtain (25). \square

The SINR of the FD monostatic radar-mode at the tBS in an ISAC network without the DTS is

$$\text{SINR}_{r,m}^{\text{no DTS}} = \frac{P_l h_{j_r} r_1^{-2\eta}}{P_l I_o + \sigma^2}. \quad (26)$$

Lemma 6: The ccdf of the FD monostatic radar-mode's SINR in an ISAC network without DTS is

$$\begin{aligned} \mathbb{P}(\text{SINR}_{r,m}^{\text{no DTS}} > \theta) &= \mathbb{E} \left[\bar{F}_{h_{j_r}} \left(\frac{\theta r_1^{2\eta}}{P_l} (P_l I_o + \sigma^2) \right) \right] \\ &= 1 - \mathbb{E}_\rho \left[\left(1 - \mathcal{L}_{I_o | \rho} (\epsilon_r \theta r_1^{2\eta}) \exp \left(\frac{-\epsilon_r \theta r_1^{2\eta} \sigma^2}{P_l} \right) \right)^{m_r} \right], \end{aligned} \quad (27)$$

where $\mathcal{L}_{I_o | \rho}(s)$ is obtained from (10).

Proof: Using (26) and along the lines of the proof of Lemma 3, we obtain (27). \square

Corollary 3: The joint SINR ccdf of the radar-mode in an ISAC network without DTS, where there is cooperation between bistatic and FD monostatic detection is

$$\begin{aligned} \mathbb{P}(\text{SINR}_{r,\text{joint}}^{\text{no DTS}} > \theta) &= \mathbb{P}(\text{SINR}_{r,b}^{\text{no DTS}} > \theta) + \mathbb{P}(\text{SINR}_{r,m}^{\text{no DTS}} > \theta) - \\ &\quad \mathbb{P}(\text{SINR}_{r,b}^{\text{no DTS}} > \theta) \mathbb{P}(\text{SINR}_{r,m}^{\text{no DTS}} > \theta). \end{aligned} \quad (28)$$

Proof: From the law of probability and independence of the two detection events (28) follows. \square

D. SINR Analysis of Radar-only Network

The SINR of the radar-mode at the tRad in a radar-only network via monostatic detection is

$$\text{SINR}^{\text{Rad-only}} = \frac{P_r h_r^2 R_r^{-2\eta}}{P_r I_r + \sigma^2} = \frac{P_r h_{j_r} R_r^{-2\eta}}{P_r I_r + \sigma^2}, \quad (29)$$

where h_r is fading coefficient from the tRad at \mathbf{o} to the tTar and the intercell interference at the tRad is $P_r I_r$. Here, $I_r = \sum_{\mathbf{x} \in \Phi_r} g_{\mathbf{x}} \|\mathbf{x}\|^{-\eta}$; since Φ_r like Φ has intensity λ , the LT of I_r is conditioned on ρ_{rad} and can be obtained from (10) as $\mathcal{L}_{I_r | \rho_{\text{rad}}}(s)$. Since $h_r \sim \exp(1)$, $h_r^2 \equiv h_{j_r}$ in (29) and we use the statistics of h_{j_r} in (7) from Proposition 3.

Lemma 7: The ccdf of the SINR at the tRad in a radar-only network is

$$\mathbb{P}(\text{SINR}_r^{\text{Rad-only}} > \theta) = \mathbb{E} \left[\bar{F}_{h_{j_r}} \left(\frac{\theta R_r^{2\eta}}{P_r} (P_r I_r + \sigma^2) \right) \right]$$

$$= 1 - \mathbb{E}_{\rho_{\text{rad}}} \left[\left(1 - \mathcal{L}_{I_r | \rho_{\text{rad}}} (\epsilon_r \theta R_r^{2\eta}) \exp \left(\frac{-\epsilon_r \theta R_r^{2\eta} \sigma^2}{P_r} \right) \right)^{m_r} \right], \quad (30)$$

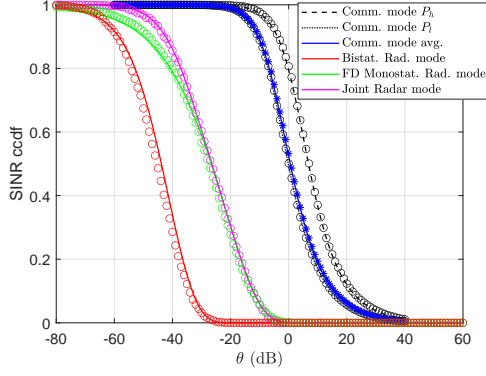
where $\mathcal{L}_{I_r | \rho_{\text{rad}}}(s)$ is obtained from (10).

Proof: Rewriting the SINR expression in (29) and using the cdf of h_{j_r} in (7) and the definition of the LT, we obtain (30). \square

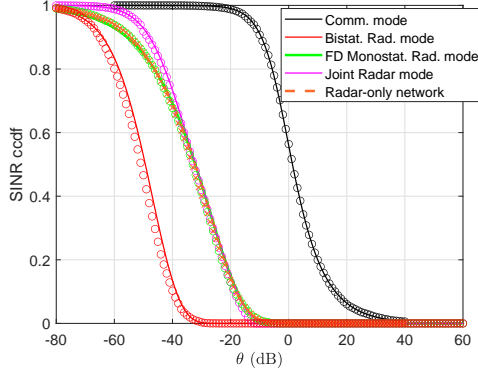
V. RESULTS

In this section, unless mentioned otherwise, we consider BS intensity $\lambda = 10^{-5}$, $\eta = 4$, $P_l = 1$ and $v = 1/(60\sqrt{\lambda})$. Simulations are repeated 10^4 times. In the ISAC network with DTS, the radar-mode is only active in slot 1 where the transmit-power is P_h and the performance is plotted accordingly. For fairness of comparison we also set $R_r = r_1$ and $P_r = P_l = 1$. Since $R_r = r_1$ and $P_r = P_l$, in this section, the performance of the radar-only network (from (30)) is identical to the performance of FD monostatic detection in the ISAC network without DTS (i.e., from (27)). This will be verified in Fig. 4 too.

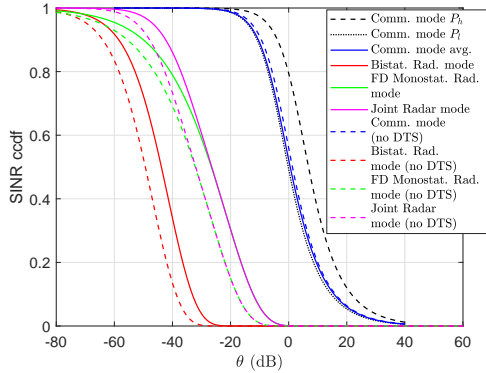
In Fig. 4 we plot the ccdf of the SINRs of interest in the ISAC network employing the DTS, the ISAC network without DTS and the radar-only network. Figs. 4a and 4b verify the accuracy of our mathematical analysis as the analytical expressions match the simulations well. As anticipated, the radar-mode in the case of both bistatic and FD monostatic detection always performs worse than its communication counterpart due to the impact of the double path-loss component; in fact, even with joint detection, the performance of the radar-mode is worse than the communication-mode highlighting the significant deterioration caused by the double path-loss. In Fig. 4b we verify that the performance of the radar-mode with FD monostatic detection in the ISAC network without DTS is identical to that in the radar-only network. This is because $P_r = P_l$ and $R_r = r_1$ in the plotted figure for fairness of comparison; however, note that in ISAC network, the radar-mode rides in the communication-mode's spectrum for free and does not require its own transmit power as it uses the cellular transmit signal. In the radar-only network, on the other hand, while we obtain the same performance as the FD monostatic ISAC without DTS, the radar-mode pays for its own spectrum and transmission power. Further, with the proposed DTS solution as well as with joint detection using the FD monostatic and bistatic detection together, we are able to improve the performance of radar detection in the ISAC network significantly more than the radar-only network. The improvement with using bistatic detection jointly with the FD monostatic detection also stems from the fact that the radar-only network (which is monostatic) suffers a double path-loss of the form $R_r^{-2\eta}$ while in the ISAC network with bistatic radar detection the path loss is of the form $R_1^{-\eta} r_2^{-\eta}$. By increasing the intensity of listening radars, which are low cost and passive, this approach in the ISAC network has the potential to control the deterioration caused by the double path loss term. This highlights the superiority of ISAC over a radar-only network not just in terms of performance improvement



(a) The ISAC network employing the DTS using $P_h = 5$ and $M = 10$.



(b) The ISAC network without DTS and the radar-only network.

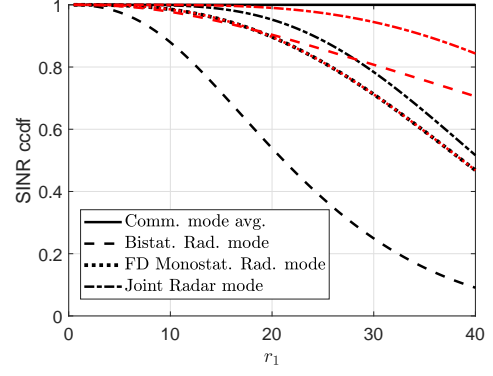


(c) The ISAC network with and without DTS (analytical only).

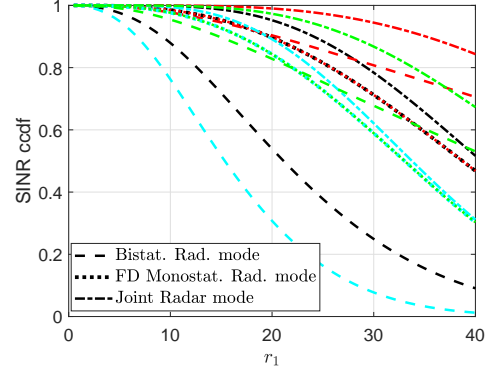
Fig. 4: The ccdf of the SIR using $r_1 = 1/(12\sqrt{\lambda})$ and $r_2 = 1/(4\sqrt{\lambda})$. Lines (markers) represent the analytical expressions (simulations).

via DTS and joint detection but also in terms of reduction of expense for both spectrum and power consumption.

In Fig. 4c we observe that, as anticipated, employing DTS improves the performance of the radar-mode; this is seen for the bistatic detection, the FD monostatic detection as well as for joint detection. The impact of employing DTS on the communication-mode is more complicated due to the trade off between improved average performance due to the higher power P_h in one slot and the increased interference for the remaining slots. We observe that the average communication-mode performance when DTS is employed for the chosen parameters is worse than the performance without DTS by less than 1 dB. On the other hand, the improvement with DTS



(a) With DTS

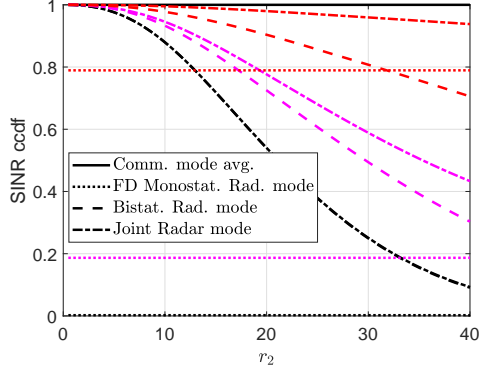


(b) With and without DTS

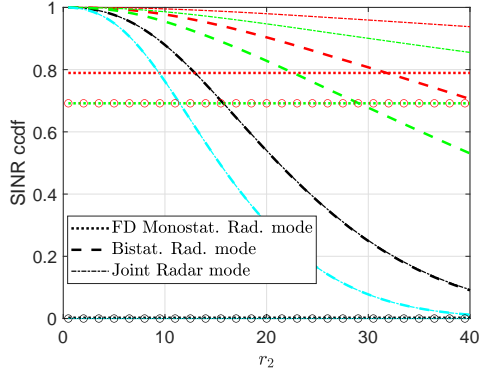
Fig. 5: Performance of the ISAC network as r_1 is increased using $\theta = -40$ dB. Black (red) lines represent $r_2 = 15v$ ($r_2 = 5v$) with DTS using $P_h = 5$ and $M = 10$. Cyan (green) lines represent $r_2 = 15v$ ($r_2 = 5v$) without DTS.

in the radar-mode is up to 5.5 dB. This highlights that with careful selection of P_h and M , DTS can result in significantly higher gains for the radar-mode than the deterioration of the communication-mode.

Fig. 5 is a plot of the SINR ccdfs in an ISAC network as r_1 is increased. We plot these with and without DTS for the radar-mode for bistatic, FD monostatic and joint detection as well as the average for the communication mode. In Fig. 5a, we observe that, as anticipated, the SINR ccdf of the communication-mode is not impacted by r_1 , while the reliability of detection in each of bistatic, FD monostatic and joint detection decrease with increasing r_1 as the path loss decreases. Further, we observe that the impact of increasing r_1 on FD monostatic detection is stronger than on bistatic detection when r_2 is small as the SINR of FD monostatic detection falls as $r_1^{-2\eta}$ while the SINR in bistatic detection only falls as $r_1^{-\eta}$. This holds true on average in general, however, when r_2 is large, due to the chosen parameters, the impact of increasing r_1 is amplified more in this case and thus for the larger r_2 in Fig. 5a we observe that the bistatic mode is impacted more by increasing r_1 . As r_2 is decreased, the performance of bistatic detection increases while the performance of FD monostatic detection remains unchanged; as a result, an increase in the performance of joint detection is also observed. In Fig. 5b, the same trends



(a) With DTS



(b) With and without DTS

Fig. 6: Performance of the ISAC network as r_2 is increased using $\theta = -40$ dB. Black (magenta, red) lines represent $r_1 = 15v$ ($r_1 = 10v$, $r_1 = 5v$) with DTS using $P_h = 5$ and $M = 10$. Cyan (green) lines represent $r_1 = 15v$ ($r_1 = 5v$) without DTS. Black (red) markers represent the radar-only network with $R_r = 15v$ ($R_r = 5v$).

are observed for the case without DTS. As anticipated, the performance of the radar-mode with DTS is always superior to its counterpart without DTS. We also note that the amount of increase in performance by incorporating DTS is roughly the same for both bistatic and FD monostatic detection as well as joint detection. This highlights the significance of using DTS to improve radar-mode performance even if only one detection technique is available.

Fig. 6 is a plot of the SINR ccdfs in an ISAC network as r_2 is increased. We plot these with and without DTS for the radar-mode for bistatic, FD monostatic and joint detection as well as the average for the communication-mode. In Fig. 6a we observe that, as anticipated, the SINR cdf of the communication-mode is not affected by increasing r_2 . Further, neither is the performance of the FD monostatic radar-detection as it is not impacted by this link distance. On the other hand, the reliability of detection of the bistatic and joint radar-mode decreases with r_2 due to the deteriorating impact of the path loss component $r_2^{-\eta}$. In the case of $r_1 = 15v$ we observe that since the FD monostatic detection reliability is very low, the joint detection is equivalent to the bistatic detection in this scenario. Decreasing r_1 improves the performance of the bistatic radar-mode as well as the FD monostatic radar-mode; the joint detection reliability in these

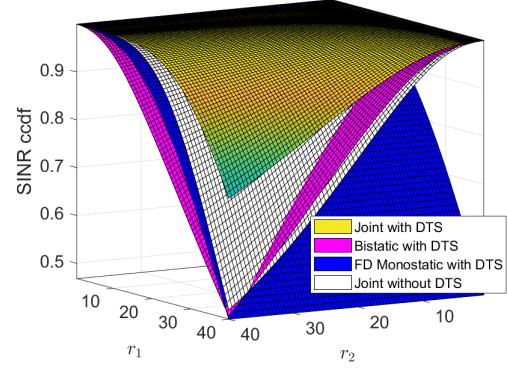
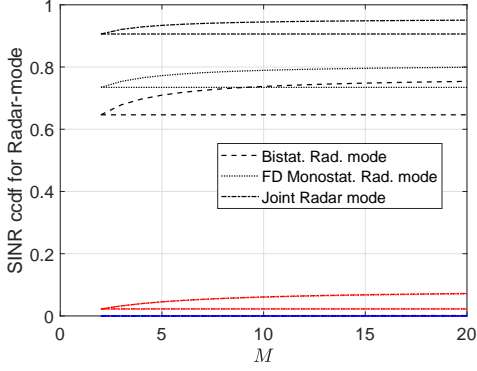


Fig. 7: Radar-mode performance vs. r_1 and r_2 using $\theta = -40$ dB. The scenario with DTS uses $P_h = 5$ and $M = 10$.

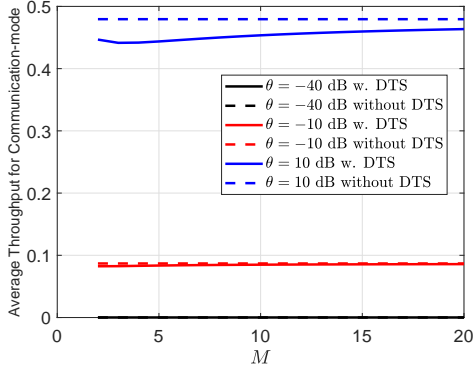
scenarios exceeds the bistatic reliability and we see a greater increase in performance of joint detection of the radar-mode than the bistatic case. In Fig. 6b, the radar performance with DTS is always superior to the performance without DTS due to the impact of the stronger signal component dominating the impact of the increased interference in the radar-mode. We also observe that FD monostatic detection using DTS (without joint detection) has better performance than the radar-only network. Further, joint detection without DTS also has better performance from the radar-only network. While the gain with using DTS is independent of r_2 , the gain from joint detection without DTS exceeds the gain from using DTS when r_2 is smaller. This highlights the improvement of our proposed solutions to enhancing radar performance. It also sheds light on the selection of a solution if only one is available: for smaller r_2 a higher gain is obtained by using joint detection and for larger r_2 DTS is superior. Of course, using both solutions results in greater gain from the radar-only network than using one solution.

In Fig. 7 we plot the SINR cdf for the bistatic, FD monostatic and joint radar-mode detection in an ISAC network with DTS vs. r_1 and r_2 . We also plot the joint radar-mode detection for the scenario without DTS. We observe that the joint detection with DTS always outperforms all of the other detection techniques. As anticipated, the surface for FD monostatic detection is unaffected by r_2 . We observe that with DTS (and without DTS, not plotted for brevity) the performance of bistatic detection dominates FD monostatic detection in some regions while the FD monostatic outperforms bistatic in other regions. Interestingly, we observe that bistatic detection with DTS is able to outperform joint detection without DTS. This observation sheds light on the fact that the DTS has potential to be even more superior to joint detection, highlighting the significance of our proposed strategy for improving the radar-mode performance for ISAC.

In Fig. 8 we plot the SINR ccdfs of the radar-mode and the average throughput of the communication-mode as performance metrics. Note that for the plotted values, the SINR cdf decreases with θ while the throughput increases. For the radar-mode in Fig. 8a, as anticipated, the performance with DTS is superior to that without DTS for each of the bistatic,



(a) Radar-mode. Curves (horizontal lines) are for the network employing DTS (without DTS). Black (red, blue) represent $\theta = -40$ dB ($\theta = -10$ dB, $\theta = 10$ dB)



(b) Communication-mode.

Fig. 8: Performance vs. M . The scenario with DTS uses $P_h = 5$.

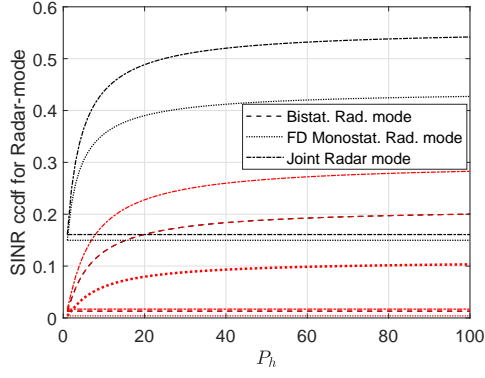
FD monostatic and joint detection cases. Further, increasing M improves radar performance with DTS for each detection technique as P_{avg} and therefore interference decrease. For each detection technique, the performance starts saturating at large M as $P_{\text{avg}} \rightarrow P_I$, which is a constant, as M grows. As anticipated, the performance without DTS is unaffected by M . Note that the performance of the radar-only network is equivalent to FD monostatic detection without DTS. For the values of r_2 in Fig. 8, bistatic detection is worse than FD monostatic and therefore the radar-only network; however, even in this scenario we observe that with joint detection, both with and without DTS, a significant improvement in performance is observed from the radar-only network.

In Fig. 8b the communication-mode throughput is plotted and we observe that the performance without DTS, which is equivalent to a traditional cellular network without ISAC, is superior to that with DTS due to the increased interference with DTS. Unlike the radar-mode, the performance difference between the two does not grow with M . In fact, we observe the existence of M where there is a throughput minima with DTS. This occurs because the communication-mode with DTS faces a trade off between the benefit from the transmission in the time slot with higher power P_h and higher interference caused by DTS. When $M = 2$, the gains from the slot with P_h dominates the deterioration from the increased interference. As M grows, the impact of the gains from the the high power

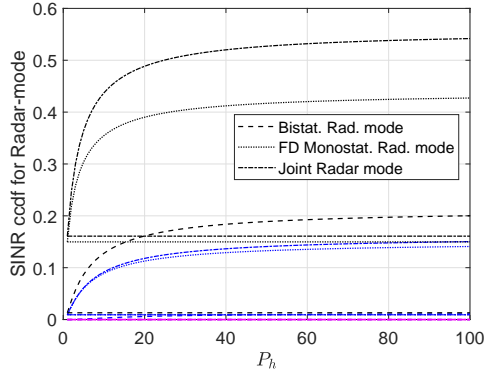
transmission decreases but so does P_{avg} and interference. At first, the impact of the decrease in gains is more and we see a drop in performance with M . After this, the impact of the decreasing P_{avg} and interference dominates and the communication-mode performance increases with M . This highlights the significance of careful selection of parameters such as M to optimize performance. Note that as M grows the performance of the communication-mode slowly grows. This indicates that with high M we can obtain good radar-mode as well as communication-mode performance. However, it ought to be mentioned that while high M improves the *quality* of radar detection, larger M reduces the *quantity* of radar detection. Parameter selection thus needs to be done as a function of both radar and communication mode quality requirements but also needs to take into account the sensing requirements of the network.

Fig. 9 plots the performance of both the communication and radar modes as P_h is increased. Increasing P_h has a trade off for both modes as the signal in slot 1 of the communication-mode and the radar-mode's signal power increase, but so does the average interference. In Figs. 9a and 9b we observe that with increasing P_h performance of the radar-mode with each of bistatic, FD monostatic and joint detection grows at first as the benefit from the increasing signal power dominates in this regime. However, at higher P_h the performance of the radar-mode starts to saturate for each detection technique. This occurs due to $P_{\text{avg}} \rightarrow P_h/M$ at large P_h . As the network being considered is large, the impact of the noise is not significant compared to the interference and an interference limited regime can be assumed (i.e., $\text{SINR} \rightarrow \text{SIR}$). At high P_h , the P_h term in the signal component and interference component cancel out and the performance of the radar-mode starts saturates with increasing P_h . Note that this performance is still superior to a radar-only network as the SINR in ISAC with DTS is amplified by M . As anticipated, the performance of the ISAC network without DTS is a lower bound on the performance with DTS and is unaffected by P_h . We also observe in Fig. 9a that interchanging the values of r_1 and r_2 (or swapping the positions of the tBS and tTar) does not impact the performance of bistatic detection as the double path loss in this scenario remains the same. However, interchanging r_1 and r_2 has a significant impact on FD monostatic detection and consequently joint detection. In particular, we observe that when r_1 is assigned the smaller value, FD monostatic and joint detection improve significantly. This sheds light on the significance of the distance r_1 which plays a larger role on radar-mode performance in ISAC than r_2 . It highlights important aspects of decision making such as using FD monostatic radar detection only when searching for targets within a certain vicinity. Another solution this highlights is to use ISAC for targets near the cell center and using traditional radar detection for cell edge targets.

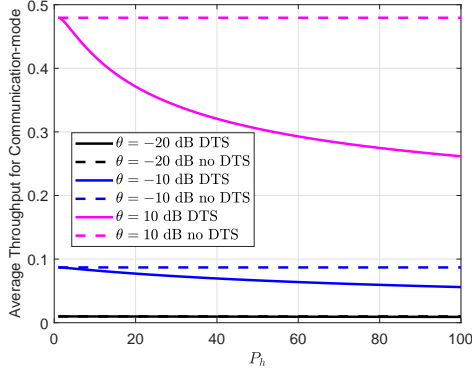
In Figs. 9b and 9c the radar-mode reliability of detection and the average communication-mode throughput are plotted vs. P_h for different θ . As expected, increasing θ reduces the radar-mode reliability for the bistatic, FD monostatic and joint detection in Fig. 9b. The communication-mode throughput on the other hand increases with θ in Fig. 9c. The performance



(a) Radar-mode with $\theta = -20$ dB. Black (red) lines represent $r_1 = 5v$ and $r_2 = 7v$ ($r_1 = 7v$ and $r_2 = 5v$).



(b) Radar-mode with DTS using $r_1 = 5v$ and $r_2 = 7v$. Black (blue, magenta) lines represent $\theta = -20$ dB ($\theta = -10$ dB, $\theta = 10$ dB).



(c) Communication-mode.

Fig. 9: Performance of the ISAC network vs. P_h . Curves (horizontal lines) are for DTS (without DTS). For the network with DTS $M = 10$.

of the communication-mode without DTS upper bounds the average performance with DTS. We observe that with DTS, the performance at first decreases slowly with P_h as the impact of the improving signal, while still not dominant, has a larger impact. As P_h grows, the impact of increasing P_h on increasing interference becomes increasingly significant, as the signal with P_h for the communication-mode is only in 1 of M slots, and the performance decreases more rapidly with P_h . At higher P_h when $P_{\text{avg}} \rightarrow P_h/M$, the throughput saturates. We again observe from Figs. 9b and 9c that with careful parameter selection the improvement in radar performance with DTS

is much more than the deterioration of the communication performance with DTS highlighting the potential of DTS as an important and practical solution to improve the performance of the radar-mode in ISAC.

VI. CONCLUSION

In this work we studied a large network employing ISAC where a single transmit signal by the BS serves both the radar and communication modes. While the communication-mode UEs have a direct link between the transmitting BS and receiving UE, the radar-mode performance is significantly more vulnerable due to the double path-loss in the signal component; this, in addition to direct links from interferers worsen the radar-mode SINR further. To combat this, we propose two solutions. First, while bistatic radar detection, where a passive radar listens for the echo from the target is more common in ISAC networks, we propose also using monostatic detection via FD at the BS. We also study the joint performance of deploying bistatic and FD monostatic detection cooperatively. Second, we propose a novel dynamic transmission strategy (DTS) to improve radar performance. Since detection may not be required in every time slot, each BS dynamically transmits with higher power P_h in one of M time slots, while it transmits with lower power P_l in the remaining slots. Since the slot with P_h is chosen at random for each BS, the average power of an interferer is P_{avg} . This way radar detection is done in the slot with P_h and since $P_{\text{avg}} < P_h$, the reduced interference further aids the radar-mode with DTS. While the DTS reduces the quantity of radar detection by $1/M$, we find that it improves quality significantly. The communication-mode faces a trade off with DTS between higher transmit power in one slot improving its performance and the increase in average interference deteriorating performance in the remaining slots as $P_{\text{avg}} > P_l$. Our results show that overall the DTS hurts the communication-mode due to higher network interference. However, the deterioration of the communication-mode is much less than the improvement of the radar-mode. We show that with careful choice of M we can reduce the deterioration of the communication-mode and improve the performance of the radar-mode at the expense of reduced quantity of detection. We also find that FD monostatic detection is the superior solution in certain scenarios like cell-center targets, while the bistatic detection is superior in other scenarios such as farther off targets. Joint detection also improves performance significantly more than either one detection technique in most situations. However, in scenarios where one of FD monostatic or bistatic dominates the other, joint detection may not be useful. Overall, we find that FD monostatic detection, joint detection and DTS are very good solutions to improve radar-mode performance in ISAC networks under different scenarios. Joint detection and DTS together can significantly improve radar performance from a traditional radar-network.

REFERENCES

- [1] J. A. Zhang, M. L. Rahman, K. Wu, X. Huang, Y. J. Guo, S. Chen, and J. Yuan, "Enabling joint communication and radar sensing in mobile networks—a survey," *IEEE Commun. Surveys and Tutorials*, vol. 24, no. 1, pp. 306–345, 2022.

- [2] J. A. Zhang, F. Liu, C. Masouros, R. W. Heath, Z. Feng, L. Zheng, and A. Petropulu, "An overview of signal processing techniques for joint communication and radar sensing," *IEEE J. Sel. Topics in Sig. Proc.*, vol. 15, no. 6, pp. 1295–1315, 2021.
- [3] S. Ram, S. Singhal, and G. Ghatak, "Optimization of network throughput of joint radar communication system using stochastic geometry," *Frontiers in Signal Processing*, vol. 2, 04 2022.
- [4] S. Yan, S. Cai, W. Xia, J. Zhang, and S. Xia, "A reconfigurable intelligent surface aided dual-function radar and communication system," in *Proc. of IEEE International Symposium on Joint Communications & Sensing (JC&S22)*, 2022, pp. 1–6.
- [5] A. Bazzi and M. Chaffi, "On outage-based beamforming design for dual-functional radar-communication 6G systems," *CoRR*, vol. abs/2207.04921, 2022. [Online]. Available: <https://arxiv.org/abs/2207.04921>
- [6] —, "On integrated sensing and communication waveforms with tunable PAPR," *CoRR*, vol. abs/2210.02892, 2022. [Online]. Available: <https://arxiv.org/abs/2210.02892>
- [7] K. S. Ali, H. ElSawy, A. Chaaban, and M. S. Alouini, "Non-orthogonal multiple access for large-scale 5G networks: Interference aware design," *IEEE Access*, vol. 5, pp. 21 204–21 216, 2017.
- [8] B. Blaszczyzyn, M. Haenggi, P. Keeler, and S. Mukherjee, *Stochastic Geometry Analysis of Cellular Networks*. Cambridge University Press, 2018.
- [9] H. ElSawy, A. Sultan-Salem, M. S. Alouini, and M. Z. Win, "Modeling and analysis of cellular networks using stochastic geometry: A tutorial," *IEEE Commun. Surveys and Tutorials*, vol. 19, no. 1, pp. 167–203, Firstquarter 2017.
- [10] P. Ren, A. Munari, and M. Petrova, "Performance tradeoffs of joint radar-communication networks," *IEEE Wireless Comm. Letters*, vol. 8, no. 1, pp. 165–168, 2019.
- [11] Z. Fang, Z. Wei, Z. Feng, X. Chen, and Z. Guo, "Performance of joint radar and communication enabled cooperative detection," in *Proc. of IEEE International Conference on Communications in China (ICCC19)*, 2019, pp. 753–758.
- [12] D. Ghoulani, A. Omri, S. Bouallegue, H. Chamkhia, and R. Bouallegue, "Stochastic geometry-based analysis of joint radar and communication-enabled cooperative detection systems," in *Proc. of International Conference on Wireless and Mobile Computing, Networking and Communications (WiMob21)*, 2021, pp. 325–330.
- [13] M. Duarte and A. Sabharwal, "Full-duplex wireless communications using off-the-shelf radios: Feasibility and first results," in *Proc. of the Forty Fourth Asilomar Conference on Signals, Systems and Computers (ASILOMAR10)*, Nov. 2010, pp. 1558–1562.
- [14] J. I. Choi, M. Jain, K. Srinivasan, P. Levis, and S. Katti, "Achieving single channel, full duplex wireless communication," in *Proc. of the Sixteenth Annual International Conference on Mobile Computing and Networking (MobiCom10)*, 2010, pp. 1–12. [Online]. Available: <http://doi.acm.org/10.1145/1859995.1859997>
- [15] K. S. Ali, H. ElSawy, and M. S. Alouini, "Modeling cellular networks with full-duplex D2D communication: A stochastic geometry approach," *IEEE Trans. Commun.*, vol. 64, no. 10, pp. 4409–4424, Oct. 2016.
- [16] C. B. Barneto, S. D. Liyanaarachchi, M. Heino, T. Riihonen, and M. Valkama, "Full duplex radio/radar technology: The enabler for advanced joint communication and sensing," *IEEE Wireless Communications*, vol. 28, no. 1, pp. 82–88, 2021.
- [17] M. Haenggi, "User point processes in cellular networks," *IEEE Wireless Comm. Letters*, vol. 6, no. 2, pp. 258–261, Apr. 2017.
- [18] A. Al-Hourani, R. J. Evans, S. Kandeepan, B. Moran, and H. Eltom, "Stochastic geometry methods for modeling automotive radar interference," *IEEE Trans. Intelligent Transportation Sys.*, vol. 19, no. 2, pp. 333–344, 2018.
- [19] S. S. Ram, G. Singh, and G. Ghatak, "Optimization of radar parameters for maximum detection probability under generalized discrete clutter conditions using stochastic geometry," *IEEE Open Jnl. Sig. Proc.*, vol. 2, pp. 571–585, 2021.
- [20] H. Alzer, "On some inequalities for the incomplete gamma function," *Mathematics of Computation*, vol. 66, no. 218, pp. 771–778, 1997. [Online]. Available: <http://www.jstor.org/stable/2153894>
- [21] M. Haenggi, "Stochastic geometry for wireless networks," *Cambridge University Press*, 2012.